Multi-scale imaging techniques to investigate solute transport across articular cartilage

Pouran, Behdad; Arbabi, Vahid; Bajpayee, A.G.; van Tiel, J; Toyras, J.; Jurvelin, J.S.; Malda, Jos; Zadpoor, Amir A.; Weinans, Harrie

DOI
10.1016/j.jbiomech.2018.06.012

Publication date
2018

Document Version
Final published version

Published in
Journal of Biomechanics

Citation (APA)
Pouran, B., Arbabi, V., Bajpayee, A. G., van Tiel, J., Toyras, J., Jurvelin, J. S., Malda, J., Zadpoor, A. A., & Weinans, H. (2018). Multi-scale imaging techniques to investigate solute transport across articular cartilage. *Journal of Biomechanics*, *78*, 10-20. https://doi.org/10.1016/j.jbiomech.2018.06.012

Journal of Biomechanics 78 (2018) 10–20

Contents lists available at ScienceDirect

Journal of Biomechanics

journal homepage: www.elsevier.com/locate/jbiomech
www.JBiomech.com

Review

Multi-scale imaging techniques to investigate solute transport across articular cartilage

Behdad Pouran [a,b], Vahid Arbabi [a,b,c], Ambika G. Bajpayee [e], Jasper van Tiel [f], Juha Töyräs [g], Jukka S. Jurvelin [g], Jos Malda [a], Amir A. Zadpoor [b], Harrie Weinans [a,b,d,*]

[a] Department of Orthopedics, UMC Utrecht, Heidelberglaan100, 3584CX Utrecht, The Netherlands
[b] Department of Biomechanical Engineering, Faculty of Mechanical, Maritime, and Materials Engineering, Delft University of Technology (TU Delft), Mekelweg 2, 2628 CD Delft, The Netherlands
[c] Department of Mechanical Engineering, Faculty of Engineering, University of Birjand, 6159175 Birjand, Iran
[d] Department of Rheumatology, UMC Utrecht, Heidelberglaan100, 3584CX Utrecht, The Netherlands
[e] Department of Bioengineering, Northeastern University, 211 Lake Hall 360 Huntington Avenue, Boston, MA 02115 MA, USA
[f] Department of Orthopedic Surgery, Erasmus MC, University Medical Center, Rotterdam, The Netherlands
[g] Department of Applied Physics, University of Eastern Finland, Kuopio, Finland

ARTICLE INFO

Article history:
Accepted 19 June 2018

Keywords:
Diffusion
Articular cartilage
Imaging
X-ray
Computed tomography
Fluorescent
MRI
Enhanced transport

ABSTRACT

As articular cartilage is an avascular tissue, the transport of nutrients and cytokines through the tissue is essential for the health of cells, i.e. chondrocytes. Transport of specific contrast agents through cartilage has been investigated to elucidate cartilage quality. In laboratory, pre-clinical and clinical studies, imaging techniques such as magnetic imaging resonance (MRI), computed tomography (CT) and fluorescent microscopy have been widely employed to visualize and quantify solute transport in cartilage. Many parameters related to the physico-chemical properties of the solute, such as molecular weight, net charge and chemical structure, have a profound effect on the transport characteristics. Information on the interplay of the solute parameters with the imaging-dependent parameters (e.g. resolution, scan and acquisition time) could assist in selecting the most optimal imaging systems and data analysis tools in a specific experimental set up. Here, we provide a comprehensive review of various imaging systems to investigate solute transport properties in articular cartilage, by discussing their potentials and limitations. The presented information can serve as a guideline for applications in cartilage imaging and therapeutics delivery and to improve understanding of the set-up of solute transport experiments in articular cartilage.

Contents

* Corresponding author at: Department of Orthopedics, UMC Utrecht, Heidelberglaan100, 3584CX Utrecht, The Netherlands.
E-mail address: h.h.weinans@umcutrecht.nl (H. Weinans).

https://doi.org/10.1016/j.jbiomech.2018.06.012
0021-9290/

1. Introduction

Articular cartilage is an avascular tissue mainly comprising large macromolecular assemblies of collagen II and aggrecans. The aggrecans contain highly negatively charged glycosaminoglycan groups (GAGs) chains, which receive their negative charges from the carboxyl and sulfate groups present in the repeating disaccharide unit of GAGs (Nia et al., 2015a,b) (Fig. 1). Solute transport in cartilage occurs through passive (Chemical potential gradient) or active (Convective interstitial fluid flow) mechanisms (Leddy and Guilak, 2003). These mechanisms determine solute's uptake and retention within the tissue extracellular matrix and their interactions with extracellular and intracellular receptors (Evans et al., 2014; Leddy and Guilak, 2003, 2008). Several previous studies have investigated the effects of solute size and charge on their ability to penetrate and reside within the articular cartilage (Arbabi et al., 2016a; Bajpayee et al., 2016; Bajpayee et al., 2015; Leddy and Guilak, 2003, 2008; Pouran et al., 2016b). Cartilage tissue has a heterogeneous structure. For example, density of negatively charged aggrecans and the spacing between collagen fibrils increase with depth, thereby resulting in depth-dependent solute diffusivities (Arbabi et al., 2015, 2016a; Leddy and Guilak, 2003; Pouran et al., 2016a). The densely packed structure of the tissue restricts the transport of most solutes due to steric hindrance, which is particularly important for larger and branched molecules (Bajpayee et al., 2015; Kokkonen et al., 2011b; Leddy and Guilak, 2008). The negative tissue charge could further slow down the transport of negatively charged solutes and prevent them from penetrating into the deeper GAG-rich regions of the tissue. This can make intra-cartilage delivery of imaging dyes and also therapeutics challenging (Arbabi et al., 2016a; Bajpayee et al., 2016; Kokkonen et al., 2016; Pouran et al., 2016b). Other parameters such as the relative volumes of solute bath and tissue, presence of stagnant solute layers at the solute bath-cartilage interface, and the diffusivity ratio of the bath to that of the cartilage were considered in experimental and numerical studies (Pouran et al., 2016a). Despite previous efforts to improve understanding the solute-tissue interactions, comprehensive guidelines to help in applying

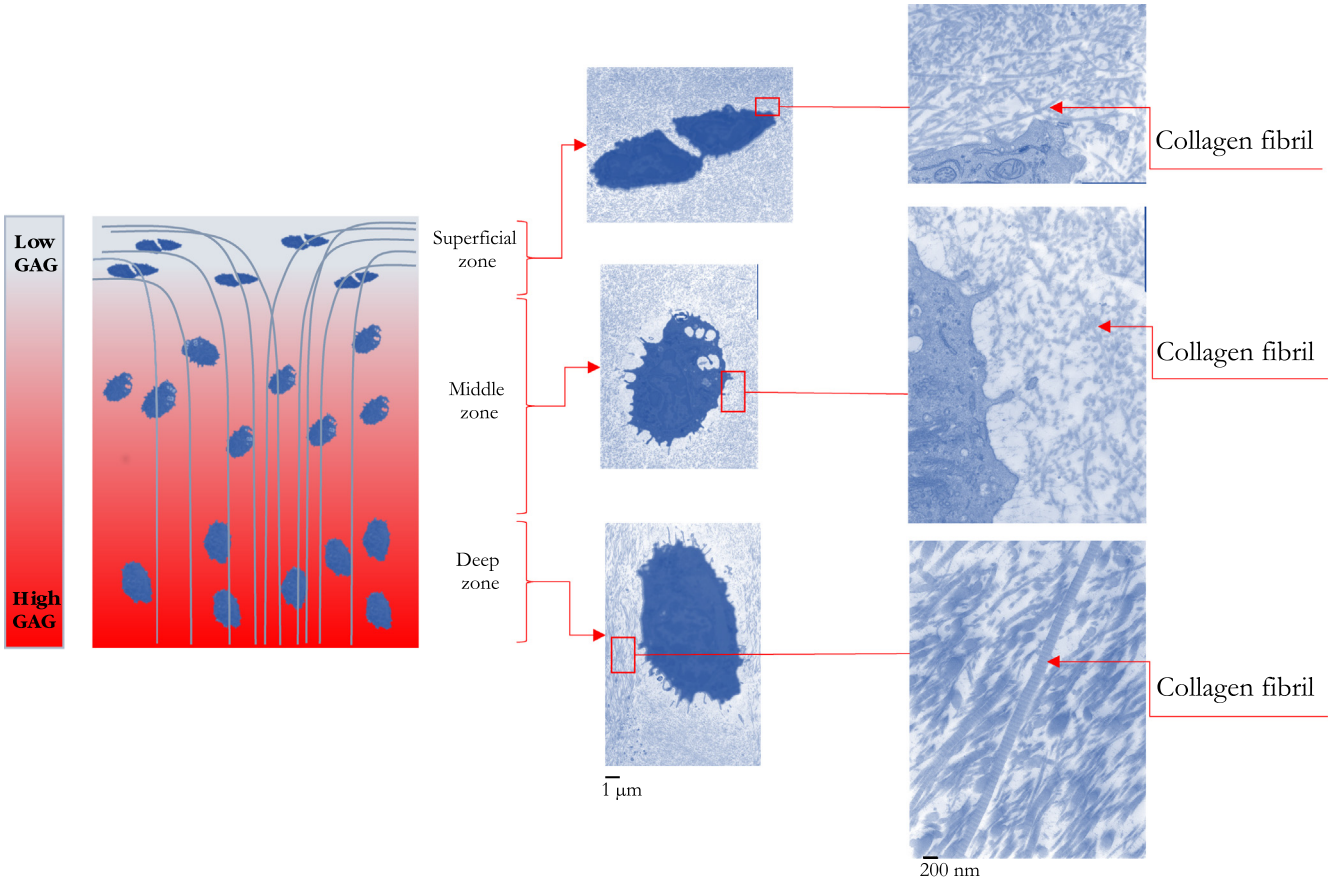

Fig. 1. Cellular information and constituents of articular cartilage: implications for solute transport. Thickness, concentration and organization of collagen fibrils, concentration and distribution of glycosaminoglycans (GAGs) as well as water content control the transport processes from the matrix side.

the above-mentioned findings and principles ex-vivo, pre-clinical, and even clinical settings are still lacking. Therefore, this review article will first introduce the transport principles essential to molecular diffusion in hydrated tissues, followed by an analysis of various imaging modalities and their applicability in studying intra-cartilage solute diffusion ex-vivo and in-vivo, as well as for clinical purposes. We will also discuss some critical considerations for setting up a transport experiment, such as the importance of tissue thickness, tissue deformation, pericellular and extracellular matrix properties, interactions with synovial fluid, external solute bath attributes, solute's charge, acquisition time, and resolution and data analysis. This review concludes by providing directions towards more efficient design of ex-vivo and in-vivo experiments and translating these considerations into clinical applications of tissue imaging and therapeutics to yield more effective results.

2. Molecular transport

2.1. Principles

Depending on the mechanical state of the tissue, both passive and active transport mechanisms take place in articular cartilage. In absence of joint motion, e.g., when the subject is relaxing or sleeping, interstitial fluid flow does not significantly affect solute transport. However, physical activities, such as jumping, climbing, cycling and running enhance interstitial fluid flow (Nia et al., 2015a), thereby increasing the transport rate of larger solutes by a factor of two (Evans and Quinn, 2006a). Fluid velocities generated at physiological conditions (1–2 μm/s) can enhance protein transport rate by up to 70-fold (Garcia et al., 1996). Moreover, the sliding motion of cartilage surfaces was shown to enhance solute transport (Graham et al., 2017). The effect of convective fluid flow is less pronounced on the transport of smaller molecules (Evans and Quinn, 2006a; Huang and Gu, 2007; O'Hara et al., 1990).

2.2. Experimental boundary conditions

Application of boundary conditions precedes the design of the diffusion experiments. The boundary conditions depend on the characteristics of the external solute bath in contact with the cartilage tissue, solute charge, loading amplitude and frequency as well as direction of solute diffusion. The concentration of the external bath may or may not change depending on whether it has finite or infinite volume as compared to the cartilage volume. Furthermore, the external bath may be well-stirred or not well-stirred, which will influence the presence and the extent of stagnant solute layers on the tissue surface (i.e. at the solute bath-tissue interface). The external bath may contain either electrically neutral or charged solutes, which create additional interactions between the bath and the ECM. Static and dynamic loading can substantially affect solute transport through alterations in the matrix compaction and modulation of fluid flow, which facilitates transport (Graham et al., 2017; Grodzinsky et al., 2000; O'Hara et al., 1990). The last boundary condition is determined by the direction of solute diffusion that may occur in axial, radial, or angular direction (or a combination of them).

In the finite-bath condition, solute concentration in the bath continuously changes with time, complicating the analysis and interpretation of the results. This setup, however, may more closely mimic the relative cartilage tissue-synovial fluid volume and the actual diffusion process in the diarthrodial joints (Arbabi et al., 2015; Pouran et al., 2016b). Thereby, it is relevant for studying intra-joint transport kinetics of therapeutics and imaging dyes following their intra-articular administration. The infinite volume condition, on the other hand, maintains constant bath solute concentration over time. Moreover, in contrast to intra-articular solute injection, systemic delivery of solutes can be best modeled using infinite bath concept since the joint capsule represents little volume as compared to the rest of the body (solute source). In both cases, constant mechanical stirring of the external bath helps to prevent the formation of stagnant solute layers at the interface of the solute bath and cartilage. Mechanical stirring could, however, cause additional fluid flow effects and result in experimental conditions that deviate from a pure diffusion model. The finite bath volume model also creates additional complexities associated with stirring limitations and the potential formation of a stagnant layer at the cartilage-bath interface. The resulting equations cannot often be solved using analytical techniques and may require advanced computational approaches.

External baths containing neutral or charged solutes behave differently, because self-repulsion within the bath and electrostatic interactions between the charged solute and proteoglycans of the ECM complicate the situation as compared to the baths that only contain neutral solutes where steric hindrance predominates.

As opposed to static compression that inhibits the penetration of solutes mainly due to increased interaction between the solute and the matrix, i.e. steric hindrance (Quinn et al., 2001), cyclic loading accelerates the transport depending on solute size, loading amplitude and frequency (Evans and Quinn, 2006b). It is worthwhile to mention that the solute transport augmentation follows a solute size-dependent trend with maximal effect on larger solutes (Garcia et al., 1996).

In the human body, articular cartilage is heterogeneously organized in direction perpendicular to its surface. As diffusion from synovial fluid to cartilage primarily occurs through the articular surface, most ex-vivo studies have designed their setups such that diffusion could only occur perpendicular to its surface. Consequently, there is limited number of studies focusing on radial and/or angular diffusive properties.

3. Imaging techniques

The development of imaging tools has enabled characterization of the diffusive behavior of solutes within articular cartilage. In fact, characterization of diffusion requires application of advanced imaging tools, such as fluorescent microscopy (Fig. 2), computed tomography (CT) (Fig. 2), and magnetic resonance imaging (MRI) (Fig. 2). Therefore, accurate characterization of the tissue requires broad knowledge of imaging techniques. In this section, we introduce and describe the principles and potentials of these imaging techniques used for cartilage imaging in particular with respect to the diffusive properties of the tissue.

3.1. Fluorescent microscopy

Primarily, two fluorescence microscopy techniques have been used to study intra-cartilage solute diffusion: scanning microphytolysis (SCAMP) and fluorescence recovery after photobleaching (FRAP). The application of SCAMP in diffusion through the pericellular matrix of articular cartilage was introduced in 2008 (Leddy et al., 2008). SCAMP works based on changes in the fluorescent signal change, which is a function of two independent variables: the rate of photobleaching and the rate of diffusion of fluorescent molecule. Molecules with fast motion traverse the laser path faster and therefore are exposed to laser path for a shorter time period, whereas slow-moving molecules are more likely to remain within the laser path and bleached. The diffusivities and bleaching constants are then obtained by fitting a 3D diffusion–reaction model to the intensity vs. time data. FRAP has been extensively used to study the diffusion of fluorescent molecules in articular cartilage

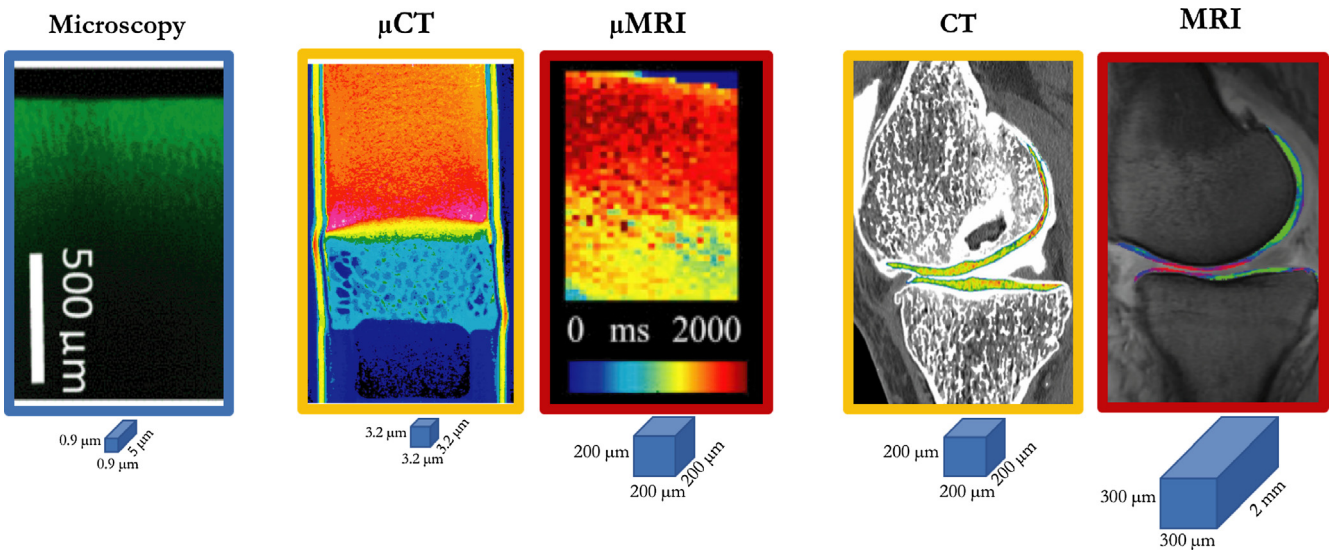

Fig. 2. Info-graph of multi-scale cartilage imaging to study solute transport across articular cartilage: implications of maximum achievable resolution and cost. Microscopy as a cost-efficient tool can be extremely beneficial for imaging the diffusion in excised tissue (Mainly 2D). CT provides high spatial resolution of the diffusion process in 3D. Clinical MRI as a costly technique suffers from poor out-of-plane resolution while in experimental setups can achieve high spatial resolution using high magnetic fields. Frame labels indicate the cost involving the equipment and infrastructure expenses: blue, yellow and red colors indicate low cost, medium and high cost, respectively (Arbabi et al., 2015; Bajpayee et al., 2014b; Rautiainen et al., 2014; Siebelt et al., 2011) (Reprint with permission from Elsevier and Wiley and ASME). (For interpretation of the references to colour in this figure legend, the reader is referred to the web version of this article.)

slices (Leddy and Guilak, 2003, 2008). A photobleached region is first created by intense laser illumination causing the fluorescence to fade away and then fluorescent molecules diffusing from the nearby region would result in gradual fluorescent recovery until complete recovery. Analytical models are then used to derive the diffusivity from the dynamic fluorescent intensity. The planar resolution of the FRAP and SCAMP has been as high as 0.9 μm^2 (Leddy and Guilak, 2003). Using confocal microscopy, these techniques can be applied to thin cartilage slices (<100 μm) allowing a z-resolution of up to a few microns (Leddy and Guilak, 2003).

In normal cartilage, diffusion in the pericellular matrix is slower than in the extracellular matrix (Leddy et al., 2008). In osteoarthritic cartilage, diffusivity of the pericellular matrix increases and becomes similar to that of the ECM (Leddy et al., 2008). Moreover, using FRAP, Leddy et al. found highest diffusion rate along the primary orientation of collagen fibrils and that diffusion anisotropy increases with the increased solute size (Leddy et al., 2006). As most of the SCAMP and FRAP setups have used 37 μm^2 large region of interest (ROI), the distance of the boundaries of the ROI from the chondrocytes (~10 μm), determines whether the measurement is performed in pericellular or extracellular matrix. SCAMP has the advantage of imaging in milli-seconds range, whereas FRAP requires several minutes. SCAMP, however, requires solving the relatively complex diffusion-reaction equations numerically, while the analytical solutions to FRAP are easily accessible in most cases. Fluorescent microscopy has also been employed to assess the effects of surface cracks on solute diffusion and adsorption properties using different sized florescent molecules in 200 μm thick cartilage slices (Chin et al., 2013; Decker et al., 2013; Moeini et al., 2014). Nevertheless, application of both FRAP and SCAMP can face limitations due to phototoxicity (high intensity laser beams) in the illuminated areas which can even affect cells about 90 μm far from the illuminated area due to light scattering (Dobrucki et al., 2007; Laissue et al., 2017). Desorption experiments (Quinn et al., 2000; Quinn et al., 2002; Shafieyan et al., 2014) were used as an indirect way to study the diffusion in cartilage where diffusion was studied from the cartilage specimen to the bath. In those experiments, the dynamic diffusion behavior in the bath in contact with cartilage containing fluorescently labeled solutes was studied.

Fluorescence correlation spectroscopy (FCS) is capable of detecting concentrations at nanomolar range (Kim et al., 2007) with applications in diffusion across normal and Trypsin-treated articular cartilage (Lee et al., 2011). FCS enables capturing the spatial and temporal information of individual molecules motion as well as the ensemble of molecules and allows to bridge the gap between those scales to quantify the diffusion process (Elson, 2011). FCS boasts the advantage of achieving diffusion information with minimum required excitation power as well as direct measurement of diffusivity within a femtoliter sized observation volume with short experiment time (~1 min) (Shoga et al., 2017). Furthermore, assumption of homogeneity in the bleached area often required by FRAP is not required using FCS. Raster image correlation spectroscopy (RICS) – an image-based extension of FCS – received considerable attention due to its sensitivity to low concentrations of fluorophore, low laser power requirement, potential to study the binding of solutes to matrix and possibility to be set up on existing conventional microscopes. RICS functions based on the moving laser beam across the sample which allows measuring the fluorescent signal (Rossow et al., 2010). Using RICS, diffusivity of multiple fluorophores ranging from 0.1 to 1000 $\mu m^2/s$ can be measured although the technique is quite time-consuming (several minutes). Shoga et al., used FCS and RICS on agarose gels and cartilage specimens and suggested that FCS can provide time-efficient assessment of microscale diffusive properties of live cartilage (low phototoxicity), whereas RICS is more appropriate to obtain tissue-averaged diffusivity in non-vital cartilage specimens (tens of minutes) (Shoga et al., 2017).

3.2. X-ray computed tomography (CT)

X-ray attenuation is a function of elemental atomic number and bulk density of the materials. Mass attenuation of cartilaginous tissues is extremely close to that of water (Lusic and Grinstaff, 2013), which complicates visualization of such hydrated tissues bathed in synovial fluid inside the joint. X-ray contrast agent molecules attenuate the X-ray signal and assist in visualizing the soft cartilaginous tissues. Computed tomography (CT) allows acquisition of three-dimensional information on the diffusion of contrast agent

molecules. Iodine (I) and Gadolinium (Gd) are well known for their X-ray attenuation characteristics and therefore vastly used to study the diffusion processes (Lusic and Grinstaff, 2013). They are used as contrast agents to visualize articular cartilage post-equilibration- the time after which no further diffusion from the source (bath) to reservoir (cartilage) takes place- and also to quantify the diffusion process through obtaining diffusivity or solute flux. Negatively charged contrast agents, e.g., ioxaglate (iodine-based) and gadopentetic acid (Gadolinium-based) (Kokkonen et al., 2016; Kulmala et al., 2010; Pouran et al., 2016b), have been applied as their interactions with proteoglycans provide quantitative essential information about the cartilage health. Positively charged iodinated contrast agents (ammonium ion. –NH3+) with different charge densities were recently introduced (Lakin et al., 2013a,b; Lakin et al., 2016) and used to enhance the retention and diffusion within articular cartilage. Nearly all above-mentioned molecules (both I-based and Gd-based) represent relatively small molecular weight (below 2 kDa). To study the effects of solute's charge on the diffusion characteristics, Pouran et al. (Pouran et al., 2016b) compared the dynamic transport of similarly sized molecules with varying net charges including iodinated molecules of ioxaglate (electrical charge = −1) and iodixanol (charge = 0) and found 2.5-fold lower ioxaglate flux in the superficial zone. The effect of cyclic mechanical loading (10% strain and 1 Hz) on patellar cartilage was underscored which resulted in more than 3-fold boost in initial contrast flux compared to passive diffusion (no loading) (voxel size = $70 \times 70 \times 100\ \mu m^3$) (Entezari et al., 2014). Mechanical injury of cartilage leads to increased flux of small negatively charged contrast agents (150–636 kDa), particularly in the early time points (until 10 min), indicating to be more sensitive to the structural damage than effective partition coefficient (Kokkonen et al., 2017). Similar study reconfirms that regardless of the size of the negatively charged contrast agent, solute flux at early times provides accurate way of identifying mechanical damage. Recently advanced finite element modeling platforms were developed to quantify diffusion behavior of charged solutes across different zones of cartilage from micro-CT data (Arbabi et al., 2016a; Arbabi et al., 2017). Furthermore, those models allowed quantification of fixed charge density across articular cartilage which highlights the merit of dynamic diffusion tests to obtain two crucial cartilage parameters. Imaging immediately after injection and 45 min after injection of combined Bismuth oxide nanoparticles (260 ± 80 nm) and ioxaglate achieved high reliability for detection of mechanical injury and enzymatic degradation of cartilage (Saukko et al., 2017). Another study, showed that at equilibrium, micro-CT signal for iodinated molecules with +4 charge correlated strongly with the intra-tissue proteoglycan content (Lakin et al., 2013b) resulting in high-quality images of cartilage in in vivo rabbit models (Stewart et al., 2013) and ex-vivo mouse models (Lakin et al., 2016) even with low iodine concentration. Cartilage attention reached above 100% of that of reservoir with CA4+ and time constants between CA4+ and ioxaglate were at all time points significantly different (Stewart et al., 2013). Most recently, application of dual-contrast (neutral and positively charged) imaging was introduced to obtain information on water content as well as fixed charge density in articular cartilage (voxel size = $25 \times 25 \times 25\ \mu m^3$) (Bhattarai et al., 2018). In-vivo research conducted on healthy and osteoarthritic knee joints of patients using clinical CT (voxel size = $0.21 \times 0.21 \times 0.40\ mm^3$) proved effective for OA identification and determination of contrast agent lifetime (Kokkonen et al., 2012). In-vivo delayed cone-beam CT after ioxaglate injection into the knee joint (voxel size = $0.20 \times 0.20 \times 0.20\ mm^3$) showed promise in low-dose radiation imaging, yet capable of detecting knee cartilage lesions accurately (Kokkonen et al., 2014; Myller et al., 2017). When using peripheral quantitative CT (pQCT) (voxel size = $0.2 \times 0.2 \times 2.3\ mm^3$), immersion of bovine osteochondral blocks in ioxaglate solution for 35.5 h allowed simultaneous morphological scoring of cartilage and subchondral bone (Aula et al., 2009). Using pQCT (voxel size = voxel size = $0.2 \times 0.2 \times 2.3\ mm^3$), dynamic diffusion of ioxaglate from cartilage surface towards cartilage deep zone and vice versa was investigated and diffusion from the cartilage surface was faster (Silvast et al., 2009). Clinically applicable CT arthrography (voxel size = $0.265 \times 0.265 \times 0.750\ mm^3$) was proposed based on the equilibrium penetration of ioxaglate by comparing the results with contrast-enhanced micro-CT (voxel size = $35 \times 35 \times 35\ \mu m^3$) (Siebelt et al., 2011). Similarly, ioxaglate partitioning experiments in 3D on ex-vivo rabbit specimens were in agreement with the 2D histological sGAG distribution for both articular cartilage and meniscus (Honkanen et al., 2016; Palmer et al., 2006). Detection of surface injuries of ex-vivo articular cartilage specimens was recently accomplished by assessing the transport kinetics of sodium iodide using high-resolution micro-CT (voxel size = $8.6 \times 8.6 \times 8.6\ \mu m^3$) (Kokkonen et al., 2016). Similar strategies employing micro-CT technique were applied to calculate the diffusivity and near-equilibrium distribution of contrast agents in healthy and non-enzymatically cross-linked ex-vivo cartilage specimens (voxel size = $30.2 \times 30.2 \times 30.2\ \mu m^3$) (Kokkonen et al., 2011b; Kulmala et al., 2013). Collagen distribution in ex-vivo non-calcified cartilage was successfully determined using micro-CT (voxel size = $3.2 \times 3.2 \times 3.2\ \mu m^3$ (Nieminen et al., 2015) and $17.4 \times 17.4 \times 17.4\ \mu m^3$ (Karhula et al., 2017)) after equilibration with phosphotungstic acid and phosphomolybdic acid). Most recently, contrast-enhanced micro-CT with high spatial resolution (voxel size = $3.0 \times 3.0 \times 3.0\ \mu m^3$) has proven advantageous for assessing GAG content of murine articular cartilage but was not accurate enough to measure cartilage thickness (Mashiatulla et al., 2017). The studies on diffusion involving CT techniques have used a wide range of voxel sizes ranging between approximately $0.2 \times 0.2 \times 2.3\ mm^3$ and $3.0 \times 3.0 \times 3.0\ \mu m^3$, indicating the feasibility of CT contrast agent imaging in laboratory, pre-clinical and clinical studies.

The thickness of articular cartilage varies between different species, anatomical locations, and cartilage health conditions. Cartilage can be as thin as 100 μm in mice, up to 2.5 mm in humans and 3 mm in African elephant (Malda et al., 2013). This wide variation implies that studying the solute diffusion in different zones of cartilage particularly for thin specimens requires the highest possible resolutions. Moreover, the scan time of a particular micro-CT setup could be an issue for diffusion studies especially when scans have to be repeated multiple times. For ex-vivo experiments, bath volume, bath concentration, and presence of stagnant layers at the cartilage-bath interface are other contributing factors. These factors influence the choice of the best imaging tool and are discussed in more detail below.

3.3. Magnetic resonance imaging (MRI)

Hydrogen ions (protons) residing e.g. in water molecules and proteins are major constituents of soft tissues like articular cartilage. As MRI-images are based on the variations in relaxation times due to differences in response of hydrogen atoms in an externally applied magnetic field, it is possible to acquire depth-dependent information on the composition and structure of extracellular matrix in articular cartilage. Three major relaxation times, namely T1 (spin-lattice relaxation time), T2 (spin-spin relaxation time) and T1ρ (spin-lattice relaxation time in the rotating frame) have been used in both clinical and experimental studies. T2 relaxation anisotropy, due to proton-collagen interactions, varies depth-wise and relates to depth-dependent organization of collagen network. On the contrary, T1 relaxation is much more isotropic in articular cartilage and is known to be isotropic to the magnetic field direction.

T1 becomes important when imaging articular cartilage with paramagnetic Gd-DTPA^{2-} that shortens the T1 relaxation (Allen et al., 1999; Bashir et al., 1996; Donahue et al., 1994). This protocol is often referred to as the Delayed Gadolinium Enhanced Magnetic Resonance Imaging of cartilage or dGEMRIC. T1 is dependent on the strength of spin-lock field. When the field approaches zero, it approaches T2 relaxation and when the field increases, it becomes less anisotropic. As the main focus of the present paper is the diffusion in articular cartilage, we focus on the MRI techniques useful for diffusion studies, namely dGEMRIC, Sodium (^{23}Na), and diffusion weighted imaging (DWI).

The partitioning of Gd-DTPA^{2-} results from its interactions with negatively charged GAGs. Thereby, degeneration of cartilage, characterized by the decreased GAG content, increases the Gd-DTPA^{2-} partitioning. This leads to low T1 values (Ronga et al., 2014). Gd-DTPA^{2-} could be administered either intravenously or intraarticularly, which generates two different mechanisms for diffusion. To a large extent, the former contributes to diffusion by both direct diffusion from the synovial fluid (SF) and perfusion from the subchondral bone, whereas the latter takes place by the direct diffusion from SF to the cartilage. However, it should be noted that diffusion across the subchondral bone plate for small molecules has been recently confirmed (Pouran et al., 2017) and therefore it can also take place post-intravenous injections, which would depend on the micro-architecture of the subchondral bone plate, i.e. porosity and thickness (Arbabi et al., 2016b; Pouran et al., 2017). In MRI, the highest achievable resolution, particularly in the z-direction (direction of main magnetic field), is limited due to relatively low magnetic fields (1.5 and 3 T), which tremendously reduces the SNR (Hawezi et al., 2016; Lattanzi et al., 2014). In clinical settings, voxel sizes up to 0.40 × 0.40 × 3 mm^3 have typically been used. Dynamic ex-vivo dGEMRIC MRI (cartilage thickness of up to 2.1 mm, infinite bath, 9.4 T) was performed over 18 h to measure the diffusivity and depth-wise distribution of Gd-DTPA^{2-} in healthy and enzymatically degraded bovine articular cartilage (voxel size = 78 μm × 78 μm × 1 mm) (Salo et al., 2012). They found a trend towards higher diffusivity of Gd-DTPA^{2-} (546 Da, q = -2) through cartilage surface than through the deep zone of cartilage similar to (Silvast et al., 2009), which used ioxaglate (1269 Da, q = −1), and no significant difference in the diffusion behavior between intact and degraded samples. Application of three negatively charged and one neutral MR contrast agents with both T1 and T2 sequences (1.5 T, voxel size = 300 μm × 300 μm × 2mm) highlighted that charge of the contrast agent only controls the amount of contrast agent and not the spatial distribution of contrast agent. The authors also found that the rate of relaxation (ΔR1 and ΔR2) for both sequences were of the same magnitude for all tested contrast agents (Wiener et al., 2007). Sweeping imaging with Fourier's transformation (SWIFT, scan time = 185.5 min, isotropic voxel size = 117 × 117 × 117 μm^3, 9.4 T) was developed to generate T1-relaxation time maps of enzymatically treated and non-treated osteochondral plugs (Nissi et al., 2014). A comparative study confirmed the superiority of Gd-DTPA^{2-} over single negatively charged contrast agents for evaluation of GAG content at early diffusion times (90 min and 120 min), however Gd-BOPTA^{2-} did provide higher contrast, suggesting an alternative for the conventional dGEMRIC (Kang et al., 2017). They also appreciated the fact that volume ratio of the contrast agent solution to cartilage as well as cartilage thickness affect the diffusion kinetics. Diffusivity values of Gd-DTPA^{2-} and Gadoteridol (similar size but neutral) was slightly higher in trypsinized cartilage than those of intact cartilage, whereas only equilibrium concentration of Gd-DTPA^{2-} was sensitive to trypsinization treatment owing to its higher interaction with the GAGs (Gillis et al., 2002). Cationic Gd-based contrast agent (net charge = +4) was synthesized and its diffusion was monitored in bovine cartilage and human finger cartilage using a 8.5 T scanner (0.2 × 0.2 × 1 mm^3, scan time = 16.5 min), which provided sufficient T1 signal at one-tenth the effective dosage of gadopentetic acid (Freedman et al., 2015). Consistently, determination of fixed charge density (FCD) of cartilage using T1 relaxation post-contrast ex-vivo has been successful (Bashir et al., 1996; Salo et al., 2012). Another strategy to determine FCD in articular cartilage is sodium MRI, which functions based on interactions between positively charged sodium and FCD of cartilage. Although non-invasive, this method was shown to suffer from intrinsically insufficient SNR in the clinical imaging, chiefly due to low concentration of ^{23}Na in articular cartilage (Trattnig et al., 2010). Using experimental μMRI (7T, 17.6 μm × 17.6 μm × 1 mm), the authors found important synergistic effects of mechanical loading and depth-wise Gd-DTPA^{2-} concentration on estimation of GAGs in healthy and degraded articular cartilage (Wang et al., 2013). The detection sensitivity of cartilage enzymatic degradation improved remarkably by performing zonal analysis using T1, T2, diffusion tensor imaging as well as gadolinium enhanced T1 (7T, 126 μm × 126 μm × 2 mm) (Fleck et al., 2017).

Diffusion weighted imaging (DWI) uses the variability of diffusive motion of water within cartilage. DWI provides promising non-invasive information about tissue composition and structure, particularly collagens and GAGs (Meder et al., 2006). Previous studies using DWI indicate that in-plane resolutions up to 78 μm^2 and slice thicknesses of 2 mm are feasible (Bajd et al., 2016).

4. Imaging considerations

Depending on the type of the instrument and the goal of the experiments, one may encounter challenges when using any of the above-mentioned imaging tools. Therefore, a general set of considerations from the authors' perspective could be insightful to facilitate proper selection of the imaging tools in diffusion studies: tissue thickness, tissue deformation, pericellular matrix and extracellular matrix, synovial fluid, bath characteristics, scan time, equipment cost and availability.

4.1. Tissue thickness

The thickness of articular cartilage not only depends on the type of the joint and anatomical location but also on the species of interest. Cartilage thickness spans a wide range from a few hundred microns, for instance in mice ~100 μm, to a few millimeters in species such as human and horse ~2 mm and elephant ~3 mm (Bajpayee et al., 2015; Malda et al., 2013). Thickness can be an important factor when choosing the imaging facility particularly when investigating zone-dependent transport properties. For example, even 9.4 T MRI provides relatively low resolutions in out-of-plane orientation (Fig. 1). (Rautiainen et al., 2016), which hampers the 3D characterizations, particularly in very thin cartilage of small animals. Therefore, for mice and rat cartilage, the preferred modalities would be either micro-CT (voxel size ~ a few microns) or fluorescent microscopy techniques (planar resolution <1 μm). Prior to the scans, the dimensions of the ex-vivo samples should sometimes be chosen optimally, particularly for the micro-CTs that their provided resolutions depend on the field of view (FOV). To study the diffusion across different zones of mice and rat cartilage, one might adopt voxel sizes less than 10 μm as this accommodates at least one voxel for the superficial zone of mice cartilage (~20 μm thickness).

To quantify the diffusion phenomena i.e. obtaining solute diffusivity and flux, estimating the equilibration time before start of the experiments seems crucial. Some studies have reported that 18–24 h is sufficient to reach equilibrium (Kokkonen et al., 2016,

2011a,b; Kulmala et al., 2013) when applying small solutes (less than 2 kDa), whereas equilibrium time was not reached even after around 48 h for other studies (Pouran et al., 2017, 2016a,b). The diffusion kinetics of Gd-BOPTA^{2-} as a potential alternative to Gd-DTPA^{2-} was also believed to depend on cartilage thickness (Kang et al., 2017). In fact, diffusion-binding kinetics scales as square of the tissue thickness (l) i.e. retention time = l^2/D where D is the diffusivity (Bajpayee et al., 2014a, 2015). The key elements that play a role are the thickness of the tissue as well as integrity and density of the matrix, which exhaust solute transport through frictional loss, i.e., steric hindrance.

4.2. Tissue deformation

As cartilage contains high negative charge, it can easily undergo osmotic-induced deformations, which depend on the osmolality of the external bath. Some diffusion experiments, similar to (Pouran et al., 2016b), cause deformations that must be accounted for before proceeding to image processing. The above-mentioned work and similar studies (Pouran et al., 2016b; Silvast et al., 2013) have reported deformations of about 5–8%, which for a 2.7 mm thick cartilage means ~200 μm. A minimum spatial resolution of 200 μm is therefore recommended. As this resolution should be applied out-of-plane, application of MRI techniques would be limited although high field MRI (7T) achieves satisfactory in-the-plane resolution (Fleck et al., 2017). Visualization of the tissue deformation during the diffusion process is also challenging using fluorescent-based techniques. Then, according to the presented resolutions earlier, the only robust technique for this particular case would be micro-CT which benefits from high spatial resolution and relatively short scan times.

4.3. Extracellular matrix and pericellular matrix

Due to higher charge and density of PCM in healthy cartilage, the diffusive properties of PCM could be distinctly different from those of ECM. Proper understanding of PCM diffusive properties requires imaging tools with resolutions in the order of a few microns, thereby necessitating application of ultra-high resolution micro-CTs (~10 μm^3 voxel size) and fluorescent techniques. Fluorescent techniques boast the advantage that diffusion of larger molecules (>2 kDa) and perhaps more clinically relevant molecules could more conveniently be studied. Obviously, MRI techniques could not be used to study diffusion in PCM.

4.4. Synovial fluid

The volume, viscosity, and composition of the synovial fluid could potentially influence solute transport. The required amount of diffusing molecule for either visualization or therapeutic purposes, or in other words, solute concentration in the joint could influence the solute distribution within the cartilage, especially if the diffusing molecule is charged (Arbabi et al., 2016a; Pouran et al., 2016a). This is even more important if the diffusing molecule is negatively charged and therefore charge-driven transport plays a role (Arbabi et al., 2016a). Moreover, injected solute concentration and synovial fluid osmolality are inter-related and therefore tissue swelling/shrinkage is expected, which requires attention to be paid prior to the scans. If the injection volume is too low, solute transport could be adversely affected because of lack of sufficient transport to deeper zones. On the contrary, if the injection volume is too high, the osmolality may rise, causing tissue deformation, which complicates the post-processing. Viscosity and composition of the synovial fluid are two major factors that change during the disease progression and could alter the solute transport features, e.g., by formation of undesirable stagnant layers near the cartilage surface.

4.5. External bath attributes

Some of important factors that control solute penetration are the solute molecular size, stirring conditions, and concentration of the bath. In CT-based experiments, large and particularly concentrated baths could cause considerable beam hardening (X-ray spectrum shape changes), which creates artefacts in the resulting images. The orientation of the bath with respect to the cartilage specimen is crucial in MRI experiments. The stirring of the bath has been suggested to minimize the unfavorable effects of stagnant layer at the cartilage-bath interface. Although gentle stirring, particularly when the mechanical stirrer is kept far enough from the cartilage surface, inhibits the formation of the stagnant layer (Garcia et al., 1996), it could also influence solute transport through eddy formation, i.e., a convective flow near the cartilage surface. The concept of finite bath was introduced to reduce the consumption of contrast agent and associated beam hardening (Arbabi et al., 2015; Pouran et al., 2016b). Moreover, the minimum bath size to sufficiently feed the deep zones of cartilage could be determined using advanced computational techniques (Pouran et al., 2016a). The ratio of solute diffusivity in the bath to that of the cartilage has been also shown to be critical (Pouran et al., 2016a). Using confined volumes of external bath enables studying the actual diffusive behavior of cartilage in the confined joint space. The concentration of the applied bath affects the diffusion in two ways: (1) possible deviations from the Fick's assumption particularly in baths containing charged particles (charge repulsion-assisted transport) and (2) increased osmolality that affects the compaction of the matrix components which may affect the transport (Pouran et al., 2016b). The associated complexities involved in some baths, such as those discussed, could be overcome through application of computational methods.

4.6. Image acquisition

The scan time is of utmost importance in CT- and MRI-, and fluorescent-based diffusion experiments. Recording the solute diffusion during the first few minutes after exposing the cartilage to the bath may be critical to determine the solute diffusivity and/or solute flux in the superficial zone (i.e. the first ~20% of the entire cartilage thickness). Then, the short scan times that have become available through sophisticated CT and MRI machines are beneficial, particularly when the solute of interest is small. The required scanning time of few minutes to few tens of minutes required by most micro-CTs and μMRIs, respectively, may limit the imaging in such cases. Preparatory steps, such as active motion of the joints, are crucial in the clinics to allow sufficient distribution of the contrast agents into the cartilage. Although long waiting times allow for sufficient penetration of the solute, they cause faster clearance from the joint (Sigurdsson et al., 2016; Sigurdsson et al., 2014). Optimal waiting time, e.g., imaging at 120 min after injection of dGEMRIC, has been therefore applied (Sigurdsson et al., 2016).

For the CTs with spatial resolution defined by the FOV, proper selection of the dimensions of sample is needed to ensure sufficient volume coverage. Moreover, in-vivo scans of relatively large rabbits and rats, two important animal models, could be challenging as well as proper positioning of the animal to allow sufficient view of the region of interest. Therefore, scanning of injected larger joints, for instance in rabbits, may be associated with relatively lower spatial resolutions, which may impair the investigation of diffusion in different cartilage zones. Application of fluorescent microscopy obviously is limited to studying diffusion across thin

Table 1
Specifications of Fluorescent Microscopy, CT and MRI used in solute transport studies.

Imaging tool	Tissue form	Zonal/single zone	Maximum resolution	Imaging time interval	Live species	Solute size	Bath concentration limitation	PCM/ECM*	Cost
Fluorescent microscopy	Excised	Zonal	Few hundred nanometers	Tens of seconds	None	Large	No limitation	PCM and ECM	Low
Clinical CT	In-vivo, in-vitro and clinical	Thickness dependent	Few hundred microns	Tens of seconds	Except mouse and rat (cartilage thickness < spatial resolution)	Mostly small	Low to medium concentrations	ECM	Middle
Experimental CT	In-vivo and in-vitro	Zonal	Few microns	Tens of seconds	Up to rabbit size (Chamber size limitation)	Mostly small	Low to medium concentrations	PCM and ECM	Middle
Clinical MRI	In-vivo, in-vitro and clinical	Thickness dependent	Few hundred microns (2D), few millimeters thick slice	Tens of minutes	Except mouse, rat and rabbit (cartilage thickness < spatial resolution)	Mostly small	Low	ECM	High
Experimental MRI	In-vivo, in-vitro	Thickness dependent	Few microns (2D), few millimeters thick slice	Few hours	Up to rabbit size (Chamber size limitation)	Mostly small	Low	ECM	High

* PCM: Pericellular Matrix. ECM: Extracellular Matrix.

ex-vivo slices and therefore monitoring temporal diffusion behavior in 3D becomes literally infeasible.

4.7. Equipment cost

Selection criteria for the appropriate imaging tool should take instrument cost into account as well. Although the high cost of MRI systems may be seen as a disadvantage, it is counterbalanced by capability of determining the diffusion attributes of water molecules in a minimally invasive manner. On the other hand, clinical CT and micro-CT systems with lower costs allow for high-resolution 3D imaging of diffusion process. Involvement of ionizing radiation, however, could be a concern when designing animal experiments and clinical studies. Among the systems reviewed so far, the fluorescent microscopy techniques are the most accessible and cost-efficient, which also allow for studying the diffusion of a wide range of molecules.

The pros and cons as well as the selection criteria for the imaging systems discussed earlier are summarized in Table 1 and Fig. 2. Fig. 3 illustrates the different scales of imaging tools ranging from clinical to ex-vivo applications.

5. Transport augmentation

Enhancing solute transport could revolutionize drug delivery strategies as well as image acquisition technologies. The ECM of articular cartilage presents a densely-packed structure and is highly negatively charged, which hinders the transport of polymer-based therapeutics and negatively-charged solutes (Bajpayee and Grodzinsky, 2017). One way to enhance the retention of the drugs is to modify them with ligands, e.g. WYRGRL (a peptide sequence of collagen II binding domain), which binds to collagen II and allows matrix binding (Rothenfluh et al., 2008). On the other hand, the size of the particles governs their ability to penetrate through the matrix. Sufficiently small nanoparticles (<38 nm) were initially believed to diffuse across various zones of cartilage (Rothenfluh et al., 2008). However, synthesized nanoparticles often present a Gaussian size distribution, which is remarkable as a later study suggested that even 15 nm quantum dots only penetrate into a small fraction of the superficial zone after 24 h (Bajpayee et al., 2014b). The same study concluded that the transport is size- and shape-dependent. Traumatic damage of cartilage was shown to facilitate the transport of fragments of anti-inflammation therapeutics (anti-IL-6 antigen binding fragments, ~48 kDa) unlike the full-sized antibodies (Byun et al., 2013). As already mentioned, molecules larger than 15 nm experience difficulty penetrating into ECM, although positively charged gene delivery agents (i.e. self-complementary recombinant adeno-associated virus vectors) even with 20 nm size could be successfully delivered across articular cartilage of equine midcarpal joint (<1 mm thick (Lee et al., 2014))(Watson et al., 2013). Harnessing electrostatic features enabled more efficient delivery of some therapeutics, driven through an electrochemical gradient, compared to diffusion only-based delivery, e.g. Dexamethasone to the cells and matrix targets. Avidin (7 nm, 66 kDa, net charge = +20), unlike NeutroAvidin (7 nm, 60 kDa, net charge = 0) dramatically increased the retention (minimum 15 days) and uptake (400 times larger than that of NeutrAvidin) inside bovine cartilage explants owing to electrostatic partitioning and binding to ECM. Avidin was found to penetrate through full thickness rabbit cartilage and remained bound within for at least 3 weeks in an ACL-transection rabbit model of post traumatic osteoarthritis (Bajpayee et al., 2017). Consequently, positively charged Avidin was shown to deliver dexamethasone inside the cartilage, thereby controlling the cytokine induced GAG loss over a period of three

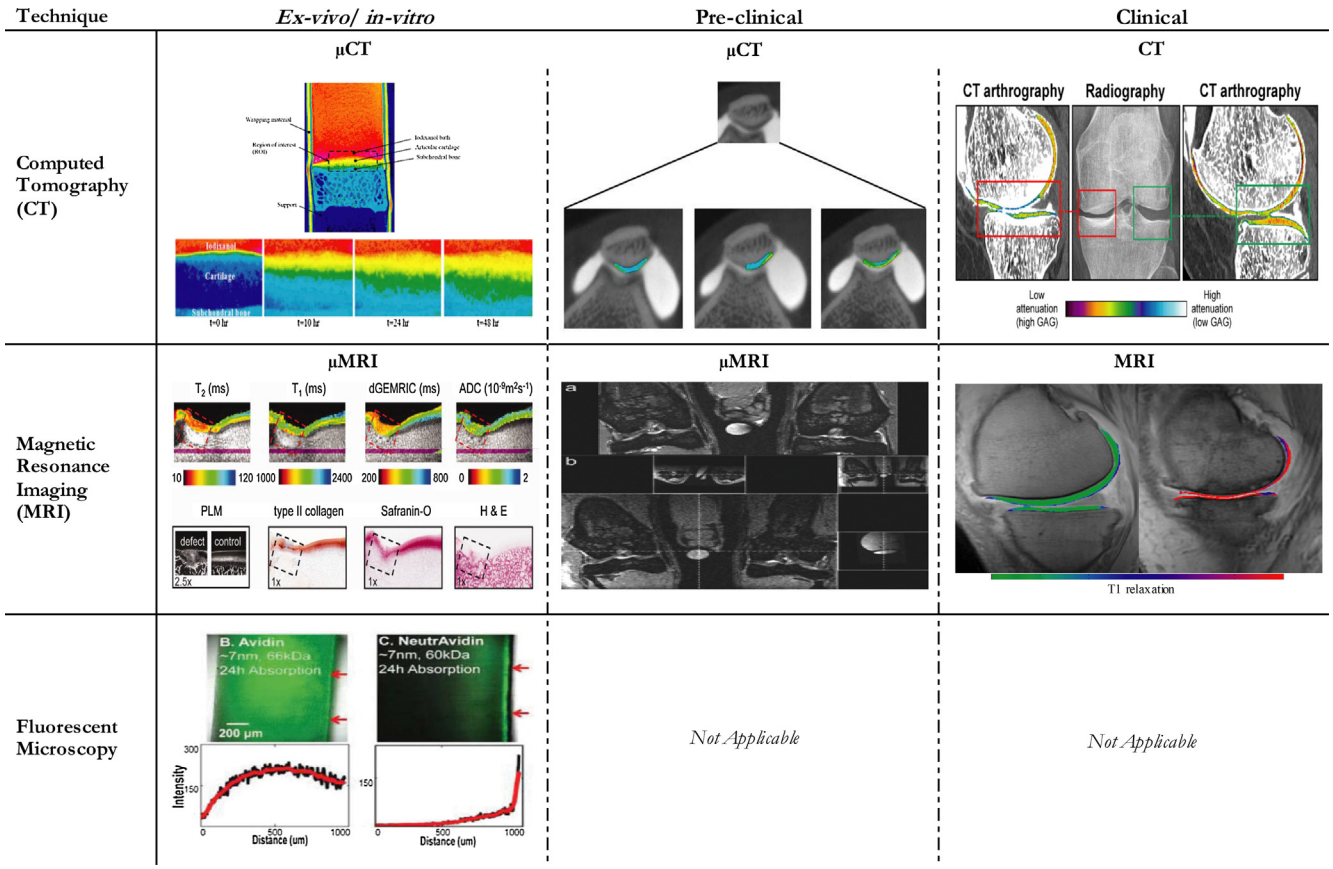

Fig. 3. Application of predominant imaging tools to study solute transport across articular cartilage (Arbabi et al., 2015; Bajpayee et al., 2014b; de Visser et al., 2017; Nieminen et al., 2012; Oei et al., 2014; Wachsmuth et al., 2003) (Reprint with permission from Elsevier, ASME and Wiley).

weeks with only a single low dose of the drug (Bajpayee et al., 2016).

6. Conclusions

This review provides an overview of the practical aspects of solute transport through articular cartilage, particularly in light of imaging perspectives in clinic and experimental setups. First, the transport mechanisms and their underlying background were reviewed and the effects of bath attributes on diffusion, which are often overlooked, were discussed. In short, fluorescent microscopy enables high-resolution diffusion of large molecules in relatively short amount of time and in different zones, as well as in pericellular matrix, although out-of-plane study is limited to few hundred microns. Instead, several thin tissue sections can be prepared and the diffusion can be monitored. Unfortunately, this inflicts disruption of tissue integrity. Advanced techniques such as FCS and RICS were recently applied to investigate the microdiffusive properties of cartilage although care should be taken to minimise potential phototoxicity. MRI has been extensively applied to measure the diffusion of typically small molecules, e.g., Gd-DTPA^{2-} and water, and high-resolution MRI substantially ameliorates the accuracy when measuring the diffusivity in 3D. However, relatively long scan times associated with this technique and low out-of-plane resolution limit its application, particularly if different zones of cartilage are studied. Even though CT-based techniques have been widely used mainly for measuring the 3D diffusivity of small iodinated molecules and offer high resolutions and short scan times, their immediate application is somewhat challenged for measuring the diffusion of larger therapeutic molecules which are often radiolucent. In the end, as delivering and retention of therapeutics have long been to high extent associated with critical challenges, guidelines with respect to namely, drug incorporation in positively charged carriers, considerations of cartilage thickness and charged bath-cartilage interactions were provided. The review, by providing sufficient tools and guidelines, can assist future research efforts on diffusion-aided cartilage imaging and quantitative characterization of solute diffusion using imaging techniques.

Acknowledgements

The authors would like to express their gratitude for the support of Dutch Arthritis Foundation (Grant No. 13-3-406) and Academy of Finland (Grant No. 269315).

Conflict of interest

The authors have nothing to declare.

References

Allen, R.G., Burstein, D., Gray, M.L., 1999. Monitoring glycosaminoglycan replenishment in cartilage explants with gadolinium-enhanced magnetic resonance imaging. J. Orthop. Res. 17, 430–436.
Arbabi, V., Pouran, B., Weinans, H., Zadpoor, A.A., 2015. Transport of neutral solute across articular cartilage: the role of zonal diffusivities. J. Biomech. Eng. 137.
Arbabi, V., Pouran, B., Weinans, H., Zadpoor, A.A., 2016a. Multiphasic modeling of charged solute transport across articular cartilage: application of multi-zone finite-bath model. J. Biomech. 49, 1510–1517.
Arbabi, V., Pouran, B., Weinans, H., Zadpoor, A.A., 2016b. Neutral solute transport across osteochondral interface: a finite element approach. J. Biomech. 49, 3833–3839.

Arbabi, V., Pouran, B., Zadpoor, A.A., Weinans, H., 2017. An experimental and finite element protocol to investigate the transport of neutral and charged solutes across articular cartilage. J. Vis. Exp.
Aula, A.S., Jurvelin, J.S., Toyras, J., 2009. Simultaneous computed tomography of articular cartilage and subchondral bone. Osteoarthr. Cartilage 17, 1583–1588.
Bajd, F., Mattea, C., Stapf, S., Sersa, I., 2016. Diffusion tensor MR microscopy of tissues with low diffusional anisotropy. Radiol. Oncol. 50, 175–187.
Bajpayee, A.G., De la Vega, R.E., Scheu, M., Varady, N.H., Yannatos, I.A., Brown, L.A., Krishnan, Y., Fitzsimons, T.J., Bhattacharya, P., Frank, E.H., Grodzinsky, A.J., Porter, R.M., 2017. Sustained intra-cartilage delivery of low dose dexamethasone using a cationic carrier for treatment of post traumatic osteoarthritis. Eur. Cell Mater. 34, 341–364.
Bajpayee, A.G., Grodzinsky, A.J., 2017. Cartilage-targeting drug delivery: can electrostatic interactions help? Nat. Rev. Rheumatol. 13, 183–193.
Bajpayee, A.G., Quadir, M.A., Hammond, P.T., Grodzinsky, A.J., 2016. Charge based intra-cartilage delivery of single dose dexamethasone using Avidin nano-carriers suppresses cytokine-induced catabolism long term. Osteoarthr. Cartilage 24, 71–81.
Bajpayee, A.G., Scheu, M., Grodzinsky, A.J., Porter, R.M., 2014a. Electrostatic interactions enable rapid penetration, enhanced uptake and retention of intra-articular injected avidin in rat knee joints. J. Orthop. Res. 32, 1044–1051.
Bajpayee, A.G., Scheu, M., Grodzinsky, A.J., Porter, R.M., 2015. A rabbit model demonstrates the influence of cartilage thickness on intra-articular drug delivery and retention within cartilage. J. Orthop. Res. 33, 660–667.
Bajpayee, A.G., Wong, C.R., Bawendi, M.G., Frank, E.H., Grodzinsky, A.J., 2014b. Avidin as a model for charge driven transport into cartilage and drug delivery for treating early stage post-traumatic osteoarthritis. Biomaterials 35, 538–549.
Bashir, A., Gray, M.L., Burstein, D., 1996. Gd-DTPA2- as a measure of cartilage degradation. Magn. Reson. Med. 36, 665–673.
Bhattarai, A., Honkanen, J.T.J., Myller, K.A.H., Prakash, M., Korhonen, M., Saukko, A.E. A., Viren, T., Joukainen, A., Patwa, A.N., Kroger, H., Grinstaff, M.W., Jurvelin, J.S., Toyras, J., 2018. Quantitative dual contrast CT technique for evaluation of articular cartilage properties. Ann. Biomed. Eng.
Byun, S., Sinskey, Y.L., Lu, Y.C., Ort, T., Kavalkovich, K., Sivakumar, P., Hunziker, E.B., Frank, E.H., Grodzinsky, A.J., 2013. Transport of anti-IL-6 antigen binding fragments into cartilage and the effects of injury. Arch. Biochem. Biophys. 532, 15–22.
Chin, H.C., Moeini, M., Quinn, T.M., 2013. Solute transport across the articular surface of injured cartilage. Arch. Biochem. Biophys. 535, 241–247.
de Visser, H.M., Weinans, H., Coeleveld, K., van Rijen, M.H., Lafeber, F.P., Mastbergen, S.C., 2017. Groove model of tibia-femoral osteoarthritis in the rat. J. Orthop. Res. 35, 496–505.
Decker, S.G., Moeini, M., Chin, H.C., Rosenzweig, D.H., Quinn, T.M., 2013. Adsorption and distribution of fluorescent solutes near the articular surface of mechanically injured cartilage. Biophys. J. 105, 2427–2436.
Dobrucki, J.W., Feret, D., Noatynska, A., 2007. Scattering of exciting light by live cells in fluorescence confocal imaging: phototoxic effects and relevance for FRAP studies. Biophys. J. 93, 1778–1786.
Donahue, K.M., Burstein, D., Manning, W.J., Gray, M.L., 1994. Studies of Gd-DTPA relaxivity and proton exchange rates in tissue. Magn. Reson. Med. 32, 66–76.
Elson, E.L., 2011. Fluorescence correlation spectroscopy: past, present, future. Biophys. J. 101, 2855–2870.
Entezari, V., Bansal, P.N., Stewart, R.C., Lakin, B.A., Grinstaff, M.W., Snyder, B.D., 2014. Effect of mechanical convection on the partitioning of an anionic iodinated contrast agent in intact patellar cartilage. J. Orthop. Res. 32, 1333–1340.
Evans, C.H., Kraus, V.B., Setton, L.A., 2014. Progress in intra-articular therapy. Nat. Rev. Rheumatol. 10, 11–22.
Evans, R.C., Quinn, T.M., 2006a. Dynamic compression augments interstitial transport of a glucose-like solute in articular cartilage. Biophys. J. 91, 1541–1547.
Evans, R.C., Quinn, T.M., 2006b. Solute convection in dynamically compressed cartilage. J. Biomech. 39, 1048–1055.
Fleck, A.K.M., Kruger, U., Carlson, K., Waltz, C., McCallum, S.A., Lucas Lu, X., Wan, L. Q., 2017. Zonal variation of MRI-measurable parameters classifies cartilage degradation. J. Biomech. 65, 176–184.
Freedman, J.D., Lusic, H., Wiewiorski, M., Farley, M., Snyder, B.D., Grinstaff, M.W., 2015. A cationic gadolinium contrast agent for magnetic resonance imaging of cartilage. Chem. Commun. (Camb.) 51, 11166–11169.
Garcia, A.M., Frank, E.H., Grimshaw, P.E., Grodzinsky, A.J., 1996. Contributions of fluid convection and electrical migration to transport in cartilage: relevance to loading. Arch. Biochem. Biophys. 333, 317–325.
Gillis, A., Gray, M., Burstein, D., 2002. Relaxivity and diffusion of gadolinium agents in cartilage. Magn. Reson. Med. 48, 1068–1071.
Graham, B.T., Moore, A.C., Burris, D.L., Price, C., 2017. Sliding enhances fluid and solute transport into buried articular cartilage contacts. Osteoarthr. Cartilage 25, 2100–2107.
Grodzinsky, A.J., Levenston, M.E., Jin, M., Frank, E.H., 2000. Cartilage tissue remodeling in response to mechanical forces. Annu. Rev. Biomed. Eng. 2, 691–713.
Hawezi, Z.K., Lammentausta, E., Svensson, J., Roos, E.M., Dahlberg, L.E., Tiderius, C.J., 2016. Regional dGEMRIC analysis in patients at risk of osteoarthritis provides additional information about activity related changes in cartilage structure. Acta Radiol. 57, 468–474.
Honkanen, J.T., Turunen, M.J., Freedman, J.D., Saarakkala, S., Grinstaff, M.W., Ylarinne, J.H., Jurvelin, J.S., Toyras, J., 2016. Cationic contrast agent diffusion differs between cartilage and meniscus. Ann. Biomed. Eng. 44, 2913–2921.
Huang, C.Y., Gu, W.Y., 2007. Effects of tension-compression nonlinearity on solute transport in charged hydrated fibrous tissues under dynamic unconfined compression. J. Biomech. Eng. 129, 423–429.
Kang, Y., Choi, J.Y., Yoo, H.J., Hong, S.H., Kang, H.S., 2017. Delayed gadolinium-enhanced MR imaging of cartilage: a comparative analysis of different gadolinium-based contrast agents in an ex vivo porcine model. Radiology 282, 734–742.
Karhula, S.S., Finnila, M.A., Lammi, M.J., Ylarinne, J.H., Kauppinen, S., Rieppo, L., Pritzker, K.P., Nieminen, H.J., Saarakkala, S., 2017. Effects of articular cartilage constituents on phosphotungstic acid enhanced micro-computed tomography. PLoS One 12, e0171075.
Kim, S.A., Heinze, K.G., Schwille, P., 2007. Fluorescence correlation spectroscopy in living cells. Nat. Methods 4, 963–973.
Kokkonen, H.T., Aula, A.S., Kroger, H., Suomalainen, J.S., Lammentausta, E., Mervaala, E., Jurvelin, J.S., Toyras, J., 2012. Delayed computed tomography arthrography of human knee cartilage in vivo. Cartilage 3, 334–341.
Kokkonen, H.T., Chin, H.C., Toyras, J., Jurvelin, J.S., Quinn, T.M., 2016. Solute transport of negatively charged contrast agents across articular surface of injured cartilage. Ann. Biomed. Eng.
Kokkonen, H.T., Chin, H.C., Toyras, J., Jurvelin, J.S., Quinn, T.M., 2017. Solute transport of negatively charged contrast agents across articular surface of injured cartilage. Ann. Biomed. Eng. 45, 973–981.
Kokkonen, H.T., Jurvelin, J.S., Tiitu, V., Toyras, J., 2011a. Detection of mechanical injury of articular cartilage using contrast enhanced computed tomography. Osteoarthr. Cartilage 19, 295–301.
Kokkonen, H.T., Makela, J., Kulmala, K.A., Rieppo, L., Jurvelin, J.S., Tiitu, V., Karjalainen, H.M., Korhonen, R.K., Kovanen, V., Toyras, J., 2011b. Computed tomography detects changes in contrast agent diffusion after collagen cross-linking typical to natural aging of articular cartilage. Osteoarthr. Cartilage 19, 1190–1198.
Kokkonen, H.T., Suomalainen, J.S., Joukainen, A., Kroger, H., Sirola, J., Jurvelin, J.S., Salo, J., Toyras, J., 2014. In vivo diagnostics of human knee cartilage lesions using delayed CBCT arthrography. J. Orthop. Res. 32, 403–412.
Kulmala, K.A., Karjalainen, H.M., Kokkonen, H.T., Tiitu, V., Kovanen, V., Lammi, M.J., Jurvelin, J.S., Korhonen, R.K., Toyras, J., 2013. Diffusion of ionic and non-ionic contrast agents in articular cartilage with increased cross-linking–contribution of steric and electrostatic effects. Med. Eng. Phys. 35, 1415–1420.
Kulmala, K.A., Korhonen, R.K., Julkunen, P., Jurvelin, J.S., Quinn, T.M., Kroger, H., Toyras, J., 2010. Diffusion coefficients of articular cartilage for different CT and MRI contrast agents. Med. Eng. Phys. 32, 878–882.
Laissue, P.P., Alghamdi, R.A., Tomancak, P., Reynaud, E.G., Shroff, H., 2017. Assessing phototoxicity in live fluorescence imaging. Nat. Methods 14, 657–661.
Lakin, B.A., Grasso, D.J., Shah, S.S., Stewart, R.C., Bansal, P.N., Freedman, J.D., Grinstaff, M.W., Snyder, B.D., 2013a. Cationic agent contrast-enhanced computed tomography imaging of cartilage correlates with the compressive modulus and coefficient of friction. Osteoarthr. Cartilage 21, 60–68.
Lakin, B.A., Grasso, D.J., Stewart, R.C., Freedman, J.D., Snyder, B.D., Grinstaff, M.W., 2013b. Contrast enhanced CT attenuation correlates with the GAG content of bovine meniscus. J. Orthop. Res. 31, 1765–1771.
Lakin, B.A., Patel, H., Holland, C., Freedman, J.D., Shelofsky, J.S., Snyder, B.D., Stok, K. S., Grinstaff, M.W., 2016. Contrast-enhanced CT using a cationic contrast agent enables non-destructive assessment of the biochemical and biomechanical properties of mouse tibial plateau cartilage. J. Orthop. Res. 34, 1130–1138.
Lattanzi, R., Petchprapa, C., Ascani, D., Babb, J.S., Chu, D., Davidovitch, R.I., Youm, T., Meislin, R.J., Recht, M.P., 2014. Detection of cartilage damage in femoroacetabular impingement with standardized dGEMRIC at 3 T. Osteoarthr. Cartilage 22, 447–456.
Leddy, H.A., Christensen, S.E., Guilak, F., 2008. Microscale diffusion properties of the cartilage pericellular matrix measured using 3D scanning microphotolysis. J. Biomech. Eng. 130, 061002.
Leddy, H.A., Guilak, F., 2003. Site-specific molecular diffusion in articular cartilage measured using fluorescence recovery after photobleaching. Ann. Biomed. Eng. 31, 753–760.
Leddy, H.A., Guilak, F., 2008. Site-specific effects of compression on macromolecular diffusion in articular cartilage. Biophys. J. 95, 4890–4895.
Leddy, H.A., Haider, M.A., Guilak, F., 2006. Diffusional anisotropy in collagenous tissues: fluorescence imaging of continuous point photobleaching. Biophys. J. 91, 311–316.
Lee, H., Kirkland, W.G., Whitmore, R.N., Theis, K.M., Young, H.E., Richardson, A.J., Jackson, R.L., Hanson, R.R., 2014. Comparison of equine articular cartilage thickness in various joints. Connect. Tissue Res. 55, 339–347.
Lee, J.I., Sato, M., Ushida, K., Mochida, J., 2011. Measurement of diffusion in articular cartilage using fluorescence correlation spectroscopy. BMC Biotech. 11, 19.
Lusic, H., Grinstaff, M.W., 2013. X-ray-computed tomography contrast agents. Chem. Rev. 113, 1641–1666.
Malda, J., de Grauw, J.C., Benders, K.E., Kik, M.J., van de Lest, C.H., Creemers, L.B., Dhert, W.J., van Weeren, P.R., 2013. Of mice, men and elephants: the relation between articular cartilage thickness and body mass. PLoS One 8, e57683.
Mashiatulla, M., Moran, M.M., Chan, D., Li, J., Freedman, J.D., Snyder, B.D., Grinstaff, M.W., Plaas, A., Sumner, D.R., 2017. Murine articular cartilage morphology and compositional quantification with high resolution cationic contrast-enhanced muCT. J Orthop. Res.

Meder, R., de Visser, S.K., Bowden, J.C., Bostrom, T., Pope, J.M., 2006. Diffusion tensor imaging of articular cartilage as a measure of tissue microstructure. Osteoarthr. Cartilage 14, 875–881.
Moeini, M., Decker, S.G., Chin, H.C., Shafieyan, Y., Rosenzweig, D.H., Quinn, T.M., 2014. Decreased solute adsorption onto cracked surfaces of mechanically injured articular cartilage: towards the design of cartilage-specific functional contrast agents. BBA 1840, 605–614.
Myller, K.A., Turunen, M.J., Honkanen, J.T., Vaananen, S.P., Iivarinen, J.T., Salo, J., Jurvelin, J.S., Toyras, J., 2017. In vivo contrast-enhanced cone beam CT provides quantitative information on articular cartilage and subchondral bone. Ann. Biomed. Eng. 45, 811–818.
Nia, H.T., Han, L., Bozchalooi, I.S., Roughley, P., Youcef-Toumi, K., Grodzinsky, A.J., Ortiz, C., 2015a. Aggrecan nanoscale solid-fluid interactions are a primary determinant of cartilage dynamic mechanical properties. ACS Nano 9, 2614–2625.
Nia, H.T., Ortiz, C., Grodzinsky, A., 2015b. Aggrecan: approaches to study biophysical and biomechanical properties. Methods Mol. Biol. 1229, 221–237.
Nieminen, H.J., Ylitalo, T., Karhula, S., Suuronen, J.P., Kauppinen, S., Serimaa, R., Haeggstrom, E., Pritzker, K.P., Valkealahti, M., Lehenkari, P., Finnila, M., Saarakkala, S., 2015. Determining collagen distribution in articular cartilage using contrast-enhanced micro-computed tomography. Osteoarthr. Cartilage 23, 1613–1621.
Nieminen, M.T., Nissi, M.J., Mattila, L., Kiviranta, I., 2012. Evaluation of chondral repair using quantitative MRI. J. Magn. Reson. Imag. 36, 1287–1299.
Nissi, M.J., Lehto, L.J., Corum, C.A., Idiyatullin, D., Ellermann, J.M., Grohn, O.H., Nieminen, M.T., 2014. Measurement of T1 relaxation time of osteochondral specimens using VFA-SWIFT. Magn. Reson. Med.
O'Hara, B.P., Urban, J.P., Maroudas, A., 1990. Influence of cyclic loading on the nutrition of articular cartilage. Ann. Rheum. Dis. 49, 536–539.
Oei, E.H., van Tiel, J., Robinson, W.H., Gold, G.E., 2014. Quantitative radiologic imaging techniques for articular cartilage composition: toward early diagnosis and development of disease-modifying therapeutics for osteoarthritis. Arthritis Care Res. (Hoboken) 66, 1129–1141.
Palmer, A.W., Guldberg, R.E., Levenston, M.E., 2006. Analysis of cartilage matrix fixed charge density and three-dimensional morphology via contrast-enhanced microcomputed tomography. Proc. Natl. Acad Sci. U.S.A. 103, 19255–19260.
Pouran, B., Arbabi, V., Bleys, R.L., Rene van Weeren, P., Zadpoor, A.A., Weinans, H., 2017. Solute transport at the interface of cartilage and subchondral bone plate: effect of micro-architecture. J. Biomech. 52, 148–154.
Pouran, B., Arbabi, V., Weinans, H., Zadpoor, A.A., 2016a. Application of multiphysics models to efficient design of experiments of solute transport across articular cartilage. Comput. Biol. Med. 78, 91–96.
Pouran, B., Arbabi, V., Zadpoor, A.A., Weinans, H., 2016b. Isolated effects of external bath osmolality, solute concentration, and electrical charge on solute transport across articular cartilage. Med. Eng. Phys. 38, 1399–1407.
Quinn, T.M., Kocian, P., Meister, J.J., 2000. Static compression is associated with decreased diffusivity of dextrans in cartilage explants. Arch. Biochem. Biophys. 384, 327–334.
Quinn, T.M., Morel, V., Meister, J.J., 2001. Static compression of articular cartilage can reduce solute diffusivity and partitioning: implications for the chondrocyte biological response. J. Biomech. 34, 1463–1469.
Quinn, T.M., Studer, C., Grodzinsky, A.J., Meister, J.J., 2002. Preservation and analysis of nonequilibrium solute concentration distributions within mechanically compressed cartilage explants. J. Biochem. Bioph. Methods 52, 83–95.
Rautiainen, J., Nieminen, M.T., Salo, E.N., Kokkonen, H.T., Mangia, S., Michaeli, S., Grohn, O., Jurvelin, J.S., Toyras, J., Nissi, M.J., 2016. Effect of collagen cross-linking on quantitative MRI parameters of articular cartilage. Osteoarthr. Cartilage 24, 1656–1664.
Rautiainen, J., Nissi, M.J., Salo, E.N., Tiitu, V., Finnila, M.A., Aho, O.M., Saarakkala, S., Lehenkari, P., Ellermann, J., Nieminen, M.T., 2014. Multiparametric MRI assessment of human articular cartilage degeneration: correlation with quantitative histology and mechanical properties. Magn. Reson. Med.
Ronga, M., Angeretti, G., Ferraro, S., DE Falco, G., Genovese, E.A., Cherubino, P., 2014. Imaging of articular cartilage: current concepts. Joints 2, 137–140.
Rossow, M.J., Sasaki, J.M., Digman, M.A., Gratton, E., 2010. Raster image correlation spectroscopy in live cells. Nat. Protoc. 5, 1761–1774.
Rothenfluh, D.A., Bermudez, H., O'Neil, C.P., Hubbell, J.A., 2008. Biofunctional polymer nanoparticles for intra-articular targeting and retention in cartilage. Nat. Mater. 7, 248–254.
Salo, E.N., Nissi, M.J., Kulmala, K.A., Tiitu, V., Toyras, J., Nieminen, M.T., 2012. Diffusion of Gd-DTPA(2)(-) into articular cartilage. Osteoarthr. Cartilage 20, 117–126.
Saukko, A.E.A., Honkanen, J.T.J., Xu, W., Vaananen, S.P., Jurvelin, J.S., Lehto, V.P., Toyras, J., 2017. Dual contrast CT method enables diagnostics of cartilage injuries and degeneration using a single CT image. Ann. Biomed. Eng. 45, 2857–2866.
Shafieyan, Y., Khosravi, N., Moeini, M., Quinn, T.M., 2014. Diffusion of MRI and CT contrast agents in articular cartilage under static compression. Biophys. J. 107, 485–492.
Shoga, J.S., Graham, B.T., Wang, L., Price, C., 2017. Direct quantification of solute diffusivity in agarose and articular cartilage using correlation spectroscopy. Ann. Biomed. Eng. 45, 2461–2474.
Siebelt, M., van Tiel, J., Waarsing, J.H., Piscaer, T.M., van Straten, M., Booij, R., Dijkshoorn, M.L., Kleinrensink, G.J., Verhaar, J.A., Krestin, G.P., Weinans, H., Oei, E.H., 2011. Clinically applied CT arthrography to measure the sulphated glycosaminoglycan content of cartilage. Osteoarthr. Cartilage 19, 1183–1189.
Sigurdsson, U., Muller, G., Siversson, C., Lammentausta, E., Svensson, J., Tiderius, C.J., Dahlberg, L.E., 2016. Delayed gadolinium-enhanced MRI of meniscus (dGEMRIM) and cartilage (dGEMRIC) in healthy knees and in knees with different stages of meniscus pathology. BMC Musculoskelet. Disord. 17, 406.
Sigurdsson, U., Siversson, C., Lammentausta, E., Svensson, J., Tiderius, C.J., Dahlberg, L.E., 2014. In vivo transport of Gd-DTPA2- into human meniscus and cartilage assessed with delayed gadolinium-enhanced MRI of cartilage (dGEMRIC). BMC Musculoskelet. Disord. 15, 226.
Silvast, T.S., Jurvelin, J.S., Lammi, M.J., Toyras, J., 2009. pQCT study on diffusion and equilibrium distribution of iodinated anionic contrast agent in human articular cartilage–associations to matrix composition and integrity. Osteoarthr. Cartilage 17, 26–32.
Silvast, T.S., Jurvelin, J.S., Tiitu, V., Quinn, T.M., Toyras, J., 2013. Bath concentration of anionic contrast agents does not affect their diffusion and distribution in articular cartilage in vitro. Cartilage 4, 42–51.
Stewart, R.C., Bansal, P.N., Entezari, V., Lusic, H., Nazarian, R.M., Snyder, B.D., Grinstaff, M.W., 2013. Contrast-enhanced CT with a high-affinity cationic contrast agent for imaging ex vivo bovine, intact ex vivo rabbit, and in vivo rabbit cartilage. Radiology 266, 141–150.
Trattnig, S., Welsch, G.H., Juras, V., Szomolanyi, P., Mayerhoefer, M.E., Stelzeneder, D., Mamisch, T.C., Bieri, O., Scheffler, K., Zbyn, S., 2010. 23Na MR imaging at 7 T after knee matrix-associated autologous chondrocyte transplantation preliminary results. Radiology 257, 175–184.
Wachsmuth, L., Keiffer, R., Juretschke, H.P., Raiss, R.X., Kimmig, N., Lindhorst, E., 2003. In vivo contrast-enhanced micro MR-imaging of experimental osteoarthritis in the rabbit knee joint at 7.1T1. Osteoarthr. Cartilage 11, 891–902.
Wang, N., Chopin, E., Xia, Y., 2013. The effects of mechanical loading and gadolinium concentration on the change of T1 and quantification of glycosaminoglycans in articular cartilage by microscopic MRI. Phys. Med. Biol. 58, 4535–4547.
Watson, R.S., Broome, T.A., Levings, P.P., Rice, B.L., Kay, J.D., Smith, A.D., Gouze, E., Gouze, J.N., Dacanay, E.A., Hauswirth, W.W., Nickerson, D.M., Dark, M.J., Colahan, P.T., Ghivizzani, S.C., 2013. scAAV-mediated gene transfer of interleukin-1-receptor antagonist to synovium and articular cartilage in large mammalian joints. Gene Ther. 20, 670–677.
Wiener, E., Woertler, K., Weirich, G., Rummeny, E.J., Settles, M., 2007. Contrast enhanced cartilage imaging: comparison of ionic and non-ionic contrast agents. Eur. J. Radiol. 63, 110–119.